Properties of superheavy nuclei with $Z = 124$

M. S. Mehta*
Department of Applied Sciences, Punjab Technical University, Kapurthala 144 601, India

Harvinder Kaur
Department of Applied Sciences, Punjab Technical University, Kapurthala 144 601, India
and Department of Physics, Rayat Bahra University, Mohali 140 104, India

Bharat Kumar† and S. K. Patra‡
Institute of Physics, Sachivalaya Marg, Bhubaneswar 751 005, India

(Received 3 August 2015; revised manuscript received 28 September 2015; published 9 November 2015)

We employ a relativistic mean field model with NL3 parametrization to investigate the ground state properties of the superheavy nucleus, $Z = 124$. The nuclei selected (from among complete isotopic series) for detailed investigation show that the nucleon density at the center is very low and therefore, these nuclei can be treated as semi-bubble nuclei. The considerable shell gap appears at neutron numbers $N = 172$, 184, and 198 showing the magicity corresponding to these numbers. The results are compared with the macro-microscopic finite range droplet model wherever possible.

DOI: 10.1103/PhysRevC.92.054305 PACS number(s): 21.10.Dr, 21.10.Ft, 21.10.Gv, 27.90.+b

I. INTRODUCTION

The location of the center of the "island of stability" and hence the next magic number for protons beyond ^{208}Pb ($Z = 82$, $N = 126$) in superheavy mass region has been debated since the prediction of the existence of long-lived superheavy nuclei in the 1960s in Refs. [1–6]. Since then significant progress has been made in the discovery of superheavy nuclei [7–9]. Experimentally, the elements up to $Z = 118$ have been synthesized to date, with half-lives varying from a few minutes to milliseconds [8]. Recently, the nuclei with $Z = 104$–118 with mass number $A = 266$–294 have been detected at Dubna [10–17] using hot fusion reactions with the neutron-rich ^{48}Ca beam on actinides targets. These measurements show the increase in half-lives with neutron number towards $N = 184$, which indicates a stable center. In more detail, the cold fusion reactions involving a doubly magic spherical target and deformed projectiles were used at GSI [7,8,18–21] to produce heavy elements up to $Z = 110$–112. At the production time of the $Z = 112$ nucleus at GSI, the fusion cross section was extremely small (1 pb), which led to the conclusion that reaching still heavier elements will be very difficult. At this time, the emergence of hot fusion reactions using ^{48}Ca projectiles at Dubna has drastically changed the situation, and nuclei with $Z = 114$–118 were synthesized and their α-decay chains also observed. The element $Z = 113$ was first reported by Oganessian *et al.* [13] and then, using cold fusion reactions, confirmed by Morita *et al.* [22,23].

But theoretically, the studies of the shell structure of superheavy nuclei in different approaches show that the magic shells beyond the spherical double-magic number ^{208}Pb ($N = 126$ and $Z = 82$), in the superheavy mass region are isotope (combination of Z and N) as well as parameter dependent. For example, recently, more microscopic calculations have predicted various other regions of stability, such as $Z = 114$, $N = 184$ [24]; $Z = 120$, $N = 172$ or 184 [25,26]; and $Z = 124$ or 126, $N = 184$ [27–29]. In the framework of relativistic continuum Hartree-Bogoliubov theory, Zhang *et al.* [30] predicted $Z = 120$, 132, and 138 with neutron numbers $N = 172$, 184, 198, 228, 238, and 258 as the next nucleon shell gaps. However, in experiments, the heaviest nucleus that could be studied so far is ^{254}No ($Z = 102$, $N = 152$) [31]. In an effort in this direction, using inductively coupled plasma-sector field mass spectroscopy, Marinov *et al.* [32] observed some neutron-deficient Th isotopes in naturally occurring thorium substances. The long-lived isomeric states, with estimated half-lives $T_{1/2} \geqslant 10^8$ yr, have been identified in the neutron-deficient ^{211,213,217,218}Th isotopes, which are associated with the superdeformed (SD) or hyperdeformed (HD) states (minima) in potential energy surfaces (PESs). In our earlier investigation [33] of $Z = 122$ isotopes ($N = 160$–198), using relativistic mean field (RMF) and Skyrme-Hartree-Fock (SHF) models, we found that the ground state solutions of some nuclei are superdeformed and/or even hyperdeformed. Of course, the SD ground state structure of superheavy nuclei were reported earlier by Ren *et al.* [34], within the theoretical framework of RMF calculations. Recently, Marinov *et al.* [35] obtained possible evidence for the existence of a long-lived superheavy nucleus with mass number $A = 292$ and atomic number $Z = 122$ or 124 in natural thorium. The half-life is again estimated to be the same as $T_{1/2} \geqslant 10^8$ yr and the abundance is (1–10) $\times 10^{12}$ as compared to ^{232}Th. This makes it interesting to make a detailed investigation of the properties of nuclei in this mass region.

In the extreme superheavy mass region, it is difficult to identify the nuclei by their α-decay chains unless a proper combination of neutron and proton closed shells is

*mehta_iop@yahoo.co.uk
†bharat@iopb.res.in
‡patra@iopb.res.in

located. Therefore, the identification of nuclei can be made through the comparison with theoretical calculations. In the present investigation we calculate the bulk properties of the $Z = 124$ nucleus within the framework of the RMF model. Here, we choose an NL3 parameter set [36] for the isotopic chain with neutron numbers $N = 158$ to $N = 220$, which encompasses the neutron numbers $N = 172$ and 184. Also, for the consistency of our results we calculate similar quantities for the isotopic chain of the $Z = 120$ nucleus.

II. FORMALISM

It has now been well established that the RMF models involving σ, ω, ρ, and photons along with the self-interactions among various mesons, i.e., the effective field theory, are very successful in explaining the structure of nuclei throughout the nuclear landscape [37–41]. The RMF model has proved to be a very powerful tool to explain the properties of finite nuclei and infinite nuclear matter [42–44] over the last three decades. We start with the modified relativistic Lagrangian density of the σ-ω model [45] for a nucleon-meson many-body system, which describes the nucleons as Dirac spinors interacting through the exchange of scalar mesons (σ), isoscalar vector mesons (ω), and isovector mesons (ρ). The scalar mesons cause attraction and the vector mesons produce repulsion, whereas the charge protons generate electromagnetic interaction.

$$\begin{aligned}\mathcal{L} = {} & \overline{\psi_i}\{i\gamma^\mu\partial_\mu - M\}\psi_i + \frac{1}{2}\partial^\mu\sigma\partial_\mu\sigma - \frac{1}{2}m_\sigma^2\sigma^2 - \frac{1}{3}g_2\sigma^3 \\ & - \frac{1}{4}g_3\sigma^4 - g_s\overline{\psi_i}\psi_i\sigma - \frac{1}{4}\Omega^{\mu\nu}\Omega_{\mu\nu} + \frac{1}{2}m_w^2V^\mu V_\mu \\ & + \frac{1}{4}c_3(V_\mu V^\mu)^2 - g_w\overline{\psi}_i\gamma^\mu\psi_i V_\mu - \frac{1}{4}\vec{B}^{\mu\nu}\cdot\vec{B}_{\mu\nu} \\ & + \frac{1}{2}m_\rho^2\vec{R}^\mu\cdot\vec{R}_\mu - g_\rho\overline{\psi}_i\gamma^\mu\vec{\tau}\psi_i - \frac{1}{4}F^{\mu\nu}F_{\mu\nu} \\ & - e\overline{\psi}_i\gamma^\mu\frac{(1-\tau_{3i})}{2}\psi_i A_\mu. \end{aligned} \quad (1)$$

The field for the σ meson is denoted by σ, that for the ω meson by V_μ, and for the isovector ρ meson by $\vec{R}_\mu$. A^μ denotes the electromagnetic field. The ψ_i are the Dirac spinors for the nucleons whose third component of the isospin is denoted by τ_{3i}. Here g_s, g_w, g_ρ, and $\frac{e^2}{4\pi} = \frac{1}{137}$ are the coupling constants for σ, ω, ρ mesons and photons, respectively. g_2, g_3, and c_3 are the parameters for the nonlinear terms of σ and ω mesons. M is the mass of the nucleon and m_σ, m_ω, and m_ρ are the masses of the σ, ω, and ρ mesons, respectively. $\Omega^{\mu\nu}$, $\vec{B}^{\mu\nu}$, and $F^{\mu\nu}$ are the field tensors for the V^μ, $\vec{R}^\mu$ and photon fields, respectively [46].

From the relativistic Lagrangian, we get the field equations for the nucleons and mesons. These equations are solved by expanding the upper and lower components of Dirac spinors and the boson fields in a deformed harmonic oscillator basis with an initial deformation. The set of coupled equations is solved numerically by a self-consistent iteration method. The center of mass motion is estimated by the usual harmonic oscillator formula $E_{\text{c.m.}} = \frac{3}{4}(41A^{-1/3})$ MeV. The quadrupole deformation parameter β_2 is evaluated from the resulting quadrupole moment [46] using the formula

$$Q = Q_n + Q_p = \sqrt{\frac{9}{5\pi}}AR^2\beta_2, \quad (2)$$

where $R = 1.2A^{1/3}$ fm. The total binding energy of the system is,

$$E_{\text{total}} = E_{\text{part}} + E_\sigma + E_\omega + E_\rho + E_c + E_{\text{pair}} + E_{\text{c.m.}}, \quad (3)$$

where E_{part} is the sum of the single-particle energies of the nucleons and E_σ, E_ω, E_ρ, E_c and E_{pair} are the contributions of the mesons fields, the Coulomb field, and the pairing energy, respectively.

For the open shell nuclei, the effect of pairing interactions is added in the BCS formalism. We consider only the $T = 1$ channel of pairing correlation, i.e., pairing between proton-proton and neutron-neutron. In such a case, a nucleon of quantum state $|j,m_z\rangle$ pairs with another nucleon having the same I_z value with quantum state $|j,-m_z\rangle$, which is the time reversal partner of the other. The RMF Lagrangian density only accommodates terms like $\psi^\dagger\psi$ (density) and no term of the form $\psi^\dagger\psi^\dagger$ or $\psi\psi$. The inclusion of a pairing correlation of the form $\psi\psi$ or $\psi^\dagger\psi^\dagger$ violates the particle number conservation [47]. Thus, a constant gap BCS-type simple prescription is adopted in our calculations to take care of the pairing correlation for open shell nuclei. The general expression for the pairing interaction to the total energy in terms of occupation probabilities v_i^2 and $u_i^2 = 1 - v_i^2$ is written as [47,48]

$$E_{\text{pair}} = -G\left[\sum_{i>0}u_i v_i\right]^2, \quad (4)$$

with $G =$ pairing force constant. The variational approach with respect to the occupation number v_i^2 gives the BCS equation [48]

$$2\epsilon_i u_i v_i - \triangle\left(u_i^2 - v_i^2\right) = 0, \quad (5)$$

with $\triangle = G\sum_{i>0}u_i v_i$.

The density with the occupation number is defined as

$$n_i = v_i^2 = \frac{1}{2}\left[1 - \frac{\epsilon_i - \lambda}{\sqrt{(\epsilon_i-\lambda)^2 + \triangle^2}}\right]. \quad (6)$$

The pairing gap (Δ) of the proton and neutron is taken from the phenomenological formula of Madland and Nix [49]:

$$\Delta_n = \frac{r}{N^{1/3}}\exp(-sI - tI^2), \quad (7)$$

$$\Delta_p = \frac{r}{Z^{1/3}}\exp(sI - tI^2), \quad (8)$$

where $I = (N - Z)/A$, $r = 5.73$ MeV, $s = 0.117$, and $t = 7.96$.

The chemical potentials λ_n and λ_p are determined by the particle numbers for neutrons and protons. The pairing energy of the nucleons using Eqs. (7) and (8) can be written as

$$E_{\text{pair}} = -\Delta\sum_{i>0}u_i v_i. \quad (9)$$

In constant pairing gap calculations, for a particular value of pairing gap Δ and force constant G, the pairing energy E_{pair} diverges if it is extended to an infinite configuration space. In fact, in all realistic calculations with finite range forces, the contribution of states of large momenta above the Fermi surface (for a particular nucleus) to Δ decreases with energy. Therefore, the pairing window in all the equations are extended up to the level $|\epsilon_i - \lambda| \leqslant 2(41A^{-1/3})$ as a function of the single particle energy. The factor 2 has been determined so as to reproduce the pairing correlation energy for neutrons in ^{118}Sn using a Gogny force [46,47,50].

III. RESULTS AND DISCUSSIONS

The superheavy nuclei $Z = 124$ with neutron numbers $N = 158$–220 are studied for the investigation of ground state properties. The results are compared with other models of previous works including the finite range droplet model (FRDM), because the experimental observations cannot be made yet at such a high Z region In numerical calculations, the number of oscillator shells for fermions and bosons $N_F = N_B = 20$ are used to evaluate the physical observables with the pairing gaps of Eqs. (7) and (8) in the BCS pairing scheme.

A. Binding energy

The binding energy of the isotopic chain of $Z = 124$ is calculated for mass number $A = 282$–384. Since there is no experimental observation for such a large Z number so far, the only comparison can be made with theoretical models such as the macroscopic-microscopic model. We compare our calculations with the finite range droplet model [51]. Here in the upper panel of Fig. 1, we compare the results (binding energy) with available FRDM results, which seem to be in good agreement. A small difference in binding energy (E_B) at the $N = 198$ region can be seen in the upper panel of Fig. 1. For example, the RMF results of binding energy and quadrupole deformation parameter for the ^{334}124 nucleus are 2284.71 MeV and $\beta_2 = 0.128$, whereas the FRDM calculations are 2286.75 MeV and $\beta_2 = 0.335$, respectively. Similarly for ^{312}124, the RMF binding energy is 2166.19 MeV and FRDM value is 2163.84 MeV with a discrepancy of 2.35 MeV. In $Z = 124$ isotopes, we get a maximum difference in binding energy of 7.43 MeV for the ^{320}124 nucleus, which is about a 0.3% discrepancy. In general, the difference in binding energy between FRDM and RMF is ∼3–4 MeV, which is reasonable in the order of two thousands magnitude. For consistency of our results, we also calculated the binding energy of the isotopic chain of $Z = 120$ which is displayed in the lower panel of Fig. 1. In this case the difference in binding energy is very small. For example, the RMF results of E_B and β_2 are 2026.51 MeV and -0.049 compared to the FRDM results of $E_B = 2023.06$ MeV and $\beta_2 = -0.104$ for ^{288}120. Similarly, the maximum discrepancy between RMF and FRDM binding energy is ∼5.83 MeV for ^{320}120.

B. Separation energy

The magic numbers in nuclei are characterized by the large shell gap in single particle energy levels. This means the nucleon in the lower level has a comparatively large value of energy than that in higher level giving, rise to more stability. The extra stability corresponding to certain numbers can be estimated from the sudden fall in the neutron separation energy. The separation energy is calculated by the difference in binding energies of two isotopes using the relation

$$S_{2n}(N,Z) = E_B(N,Z) - E_B(N-2,Z).$$

The two-neutron separation energy (S_{2n}) for the isotopic series of nuclei $Z = 124$ and 120 ($^{282-344}$124 and $^{278-340}$120) is shown in Fig. 2. The sudden fall in separation energy at $N = 172$, 184, and 198 can clearly be seen in both the cases, confirming the magic character [24–26,52] predicted in earlier studies. Although $N = 172$ is not that much pronounced in our earlier investigation of odd nuclei [52], here the magicity at $N = 172$ increases as we move to the extreme superheavy mass region [53]. Contrary to some earlier literature, there

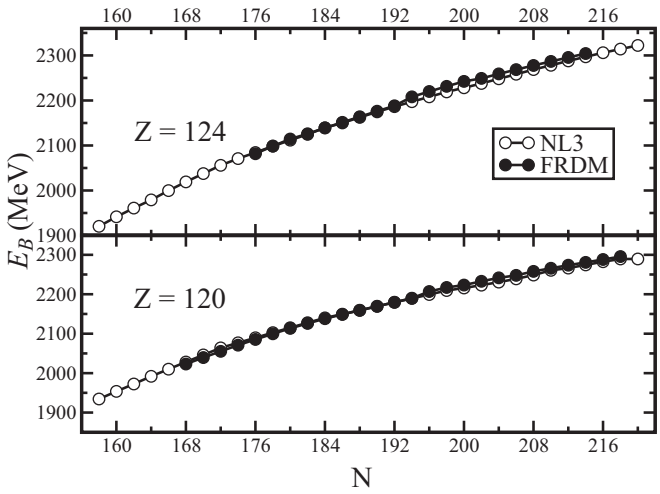

FIG. 1. Binding energy of isotopic series of nuclei $Z = 120$, 124 nuclei with NL3 parameter set.

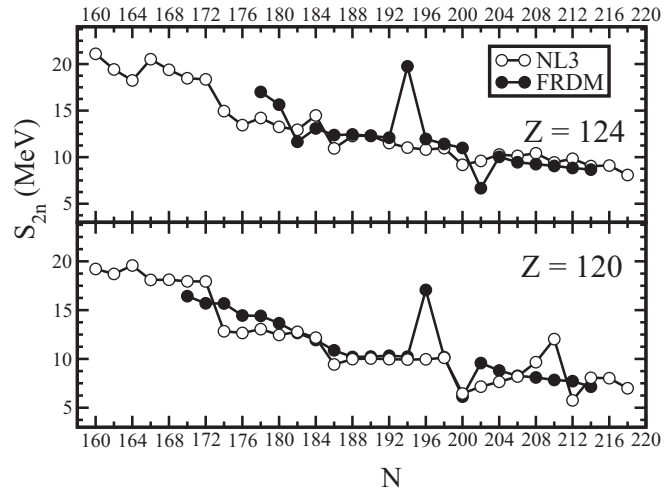

FIG. 2. Two-neutron separation energy as a function of neutron for series of $Z = 120$ and 124 nuclei.

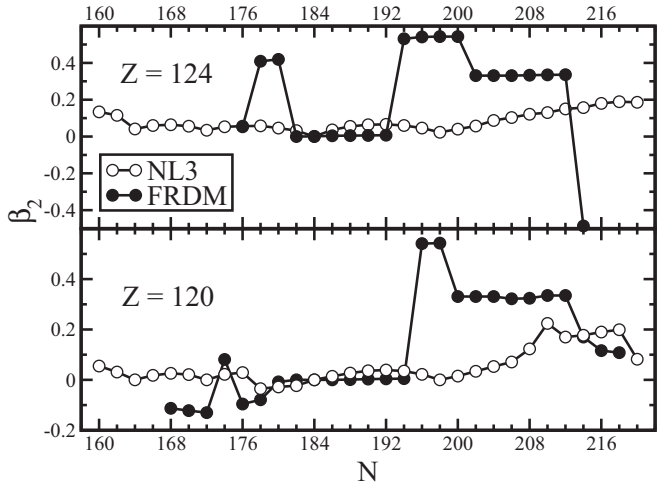

FIG. 3. Quadrupole deformation parameter β_2 for the isotopic series of $Z = 120$, 124 nuclei.

is no signature of sudden change in separation energy at the deformed magic number $N = 162$ [24] in the present calculations. The decrease in energy at $N = 172$ and 184 is ~3.5 MeV, whereas it is ~2 MeV at $N = 198$ for $Z = 124$ nuclei. In the case of $Z = 120$ isotopes the decrease in energy is ~5.0 MeV at $N = 172$, and ~3.0 and 3.5 MeV at $N = 184$ and 198, respectively. Such decrease at $N = 198$ in our calculations is nearly the same as in FRDM value. However, in FRDM the sudden decrease in separation energy appears at $N = 180$ and 200 for $Z = 124$. Except for the values at these numbers, in general all other energies from our present calculations are in good agreement (within ~2 MeV accuracy) with macro-microscopic calculations (FRDM). We observed a couple of abnormal increases in S_{2n} at ($N = 194$, $Z = 124$) and ($N = 196$, $Z = 120$), which are not seen in the present RMF calculations.

C. Quadrupole deformation parameter

The quadrupole deformation parameter β_2 gives the shape of the nuclei in the ground state. The value of β_2 is positive, negative, and zero for prolate, oblate, and spherical shapes, respectively. In our calculation shown in Fig. 3, except for a few nuclei all the isotopes of $Z = 124$ are either spherical or near spherical. The results compared with FRDM [51] agree for nuclei having $N = 176$, 182–192 as shown in the upper panel of Fig. 3. At $N = 176$ and $N = 184$ the nuclei are completely spherical. There is the least agreement beyond $N = 196$ for $Z = 124$. From the figure it is clear that the NL3 parameter set predicts the deformation parameter β_2 very close to that of FRDM at the middle mass region, i.e., from neutron numbers $N = 176$ to 192.

D. Q_α Energy and half-life (T_α)

The superheavy nuclei along the β-stability line are known to be α emitters. The α-decay half-life of the nucleus showing shell closure is believed to be comparatively larger than the neighboring nuclei. Thus, to confirm the magic number corresponding to a particular neutron number N, it is beneficial to calculate the half-life of the α decay. The investigation of the α decay of nuclei gives information about their degree of stability and possibility of existence in nature. Here we take the nucleus $^{296}124$ ($Z = 124$ and $N = 172$) for the calculation of α-decay energy [54].

The Q_α energy and half-life (T_α) are compared with available experimental data as shown in Table I. The Q_α energy is calculated using the following equation:

$$Q_\alpha(N,Z) = E_B(N,Z) - E_B(N-2,Z-2) - E_B \quad (2,2).$$

TABLE I. Q_α and T_α calculated using NL3 parameter set in RMF. The results are compared with FRDM results [51] as well as the available experimental data [55].The binding energy is in MeV and half-life is in seconds.

		RMF (NL3)			FRDM			Expt.		
A	Z	E_B	Q_α	T_α	E_B	Q_α	T_α	E_B	Q_α	T_α
296	124	2056.01	14.11	$10^{-6.41}$						
292	122	2041.83	12.98	$10^{-4.68}$						
288	120	2026.51	14.28	$10^{-7.66}$	2023.06	13.92	$10^{-7.02}$			
284	118	2012.49	13.92	$10^{-7.50}$	2008.69	13.10	$10^{-5.95}$			
280	116	1998.12	13.14	$10^{-6.54}$	1993.49	12.42	$10^{-5.10}$			
276	114	1982.96	11.88	$10.^{-4.48}$	1977.62	12.33	$10^{-5.44}$			
272	112	1966.55	11.68	$10^{-4.60}$	1961.66	11.61	$10^{-4.45}$			
268	110	1949.93	11.33	$10^{-4.38}$	1944.97	10.94	$10^{-3.47}$	1943.53	11.7	$10^{-5.2}$
264	108	1932.96	10.56	$10^{-3.14}$	1927.62	10.57	$10^{-3.18}$	1926.67	10.59	$10^{-3.2}$
260	106	1915.22	9.66	$10^{-1.42}$	1909.90	9.93	$10^{-2.15}$	1909.06	9.90	$10^{-2.07}$
256	104	1896.59	8.12	$10^{2.73}$	1891.53	8.75	$10^{0.59}$	1890.56	8.93	$10^{0.05}$
252	102	1876.41	8.33	$10^{1.25}$	1871.98	8.35	$10^{1.19}$	1871.35	8.54	$10^{0.52}$
248	100	1856.44	7.07	$10.^{5.15}$	1852.03	7.64	$10^{2.91}$	1851.57	8.0	$10^{1.60}$
244	98	1835.21	7.25	$10^{3.57}$	1831.38	6.90	$10^{5.01}$	1831.22	7.32	$10^{3.30}$
240	96	1814.17	5.93	$10^{8.68}$	1809.98	6.52	$10^{5.81}$	1810.28	6.40	$10^{6.36}$
236	94	1791.81	4.30	$10^{18.29}$	1788.21	5.77	$10^{8.54}$	1788.41	5.87	$10^{8.03}$
232	92	1767.81	3.41	$10^{25.66}$	1765.695	5.14	$10^{11.18}$	1765.98	5.41	$10^{9.50}$

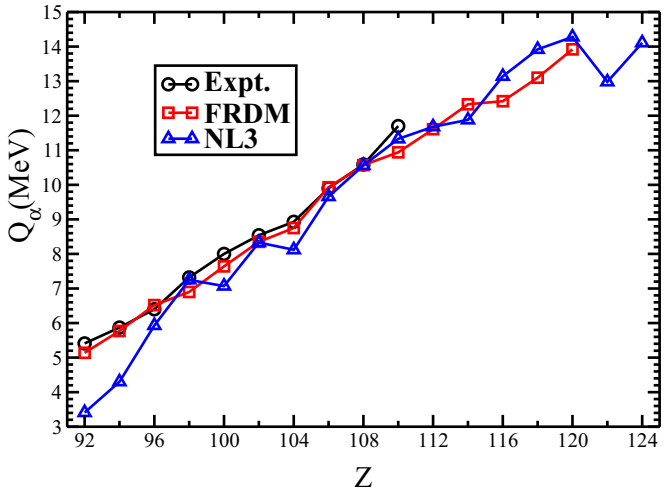

FIG. 4. (Color online) α-decay (Q_α energy) chain from $Z = 124$ to Z = 92.

In the equation, $E_B(N,Z)$ is binding energy of the parent nucleus having N neutrons and Z protons, and $E_B(N-2,Z-2)$ is the binding energy of the daughter nucleus after emission of an α particle [$E_B(2,2)$]. The binding energy of the α particle (^{4}He) is 28.296 MeV. The Q_α energy values are in good agreement with experimental data [55] as well as with FRDM [51] as shown in Table I. The decay chain is also plotted in Fig. 4 which shows good agreement with experiments as well as FRDM calculations. The half-life $\log_{10}T_\alpha$ (s) values are estimated using the phenomenological formula [56]

$$\log_{10} T_\alpha(\mathrm{s}) = \frac{aZ-b}{\sqrt{Q_\alpha}} - (cZ+d) - h_{\log},$$

where Z is the atomic number of the parent nucleus, and the other parameters are $a = 1.661\,75$, $b = 8.5166$, $c = 0.202\,28$, and $d = 33.9069$. The values of the parameters are taken from Sobiczewski *et al.* [57]. The hindrance ($h_{\log}$) caused by the odd number of protons and/or neutrons is zero here.

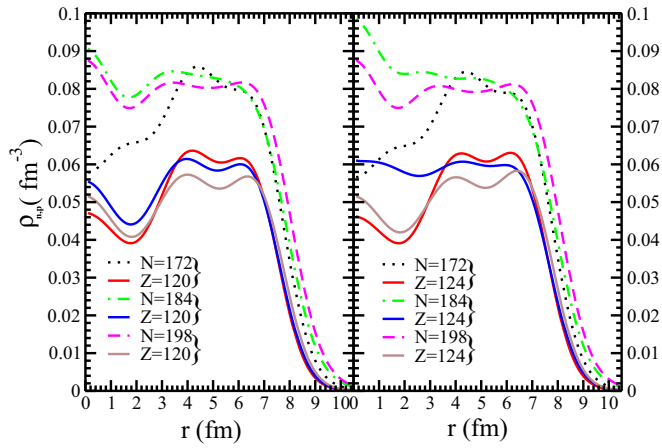

FIG. 5. (Color online) Density of selected isotopes of $Z = 120$, 124 nuclei with NL3 parameter set.

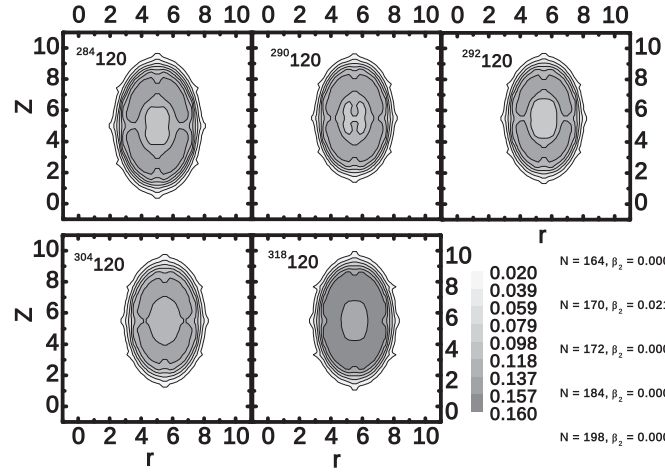

FIG. 6. Two-dimensional density contours for nuclei ^{284,290,292,304,318}120 shown using the NL3 parameter set.

E. Density distribution

The neutron and proton density distributions for $Z = 124$ and 120 nuclei are plotted in Fig. 5. The nuclei with $N = 172$, 184, and 198 are taken as representative cases for detailed investigation of the internal structure. The charge distribution of both $Z = 120$ and 124 show that the center part of nuclei have very low density indicating a hollow inside.

To gain insight into the arrangement of nucleons, we plot the two-dimensional contours for some selected nuclei. The density contours for ^{284,290,292,304,318}120 and ^{288,294,296,308,322}124 nuclei are shown in Figs. 6–8. In general, it is clear from the figures that the central regions in all nuclei except the ^{308}124 nucleus have considerably low density. For isotopes of $Z = 120$, as shown in Fig. 6, the $N = 170$ nucleus is slightly deformed ($\beta_2 = 0.021$) and all other ($N = 164$, 170, 184, and 198) are spherical in their ground state. The nuclei with $Z \geqslant 120$ have large numbers of protons and hence considerable Coulomb repulsion among protons. The strong repulsion changes the entire distribution of nucleons. The doubly magic nucleus ^{292}120 has been largely studied

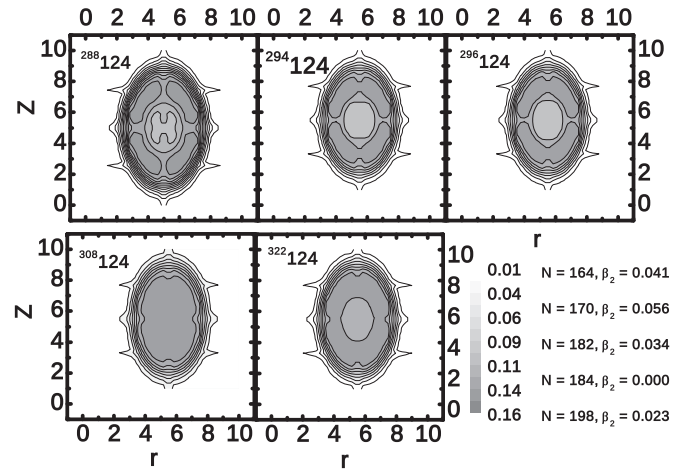

FIG. 7. Same as Fig. 6, but for nuclei ^{288,294,296,308,322}124.

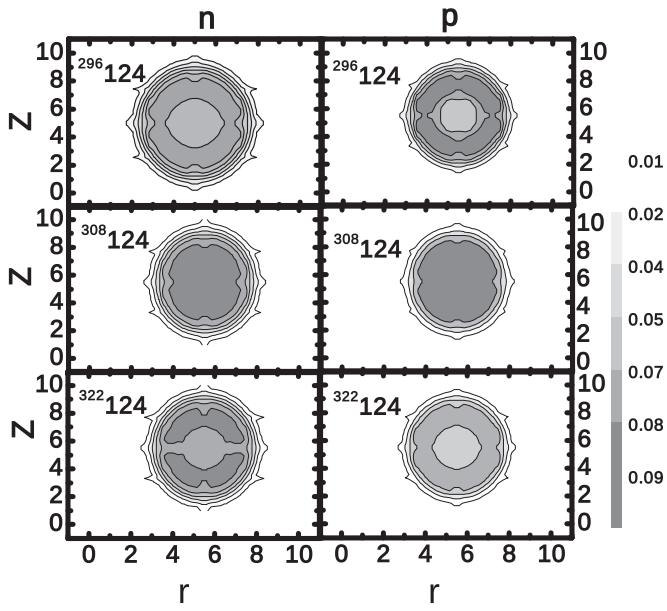

FIG. 8. Neutron and proton density distributions for nuclei $^{296,308,322}124$.

previously [58–60] and is predicted to be semi-bubble. In the present calculations using RMF (NL3), the semi-bubble structure of these nuclei can be clearly seen in Fig. 6. The hollow region at the center is spread over the radius of 1–2 fm. This may suggest that these nuclei might have a fullerene-type structure consisting of 60 α particles and a binding neutron per α and/ or few neutron clusters. The clusters of some heavier nuclei might be possible. The density distribution of $^{288,294,296,308,322}124$ nuclei is shown in Fig. 7. In this case the density of nucleus $N = 184$ is more at the central region while all other nuclei studied here are showing bubble-type structure. The low density region extends up to $\sim$2 fm. The nuclei with $N = 164$, 170, 172, and 198 are near spherical ($\beta_2 = 0.041$, 0.056, 0.034, and 0.023, respectively) whereas $N = 184$ is spherical in shape. To gain further insight into the arrangement of nucleons, we plotted the density distribution of neutrons and protons separately (Fig. 8). It is clear from the figure that both neutrons as well as protons are shifted from the central region except for the $N = 184$ nucleus.

IV. CONCLUSION

In the present work we use the RMF(NL3) model to explore the structure of the superheavy nucleus $Z = 124$. The results of our calculations are compared with macro-microscopic FRDM predictions. We calculate binding energy, quadrupole deformation parameter (β_2), two-neutron separation energy (S_{2n}), and decay half-life ($T_{1/2}$) for the isotopic series of $Z = 124$, and for consistency we calculate the same quantities for the $Z = 120$ nucleus. The quadrupole deformation parameters at the heavier side of the series show more deviation from FRDM values. The two-neutron separation energy shows a sudden fall in energy at neutron numbers $N = 172$, 184, and 198, indicating a magic structure. The α-decay energy and half-life are also calculated and compared with the experiments and FRDM results, which seem to be in good agreement. The density profile of the selected nuclei shows a depression in the density at the central region of the nuclei with the exception of $^{308}124$. This nucleus is the only candidate which does not show the depression at the center. Finally, this theoretical investigation of ground state properties of $Z = 124$ nuclei may be helpful for an experimental exploration to locate the "island of stability" which is expected to exist in the large-Z superheavy region.

[1] A. Sobiczewski, F. A. Gareev, and B. N. Kalinkin, Phys. Lett. B **22**, 500 (1966).
[2] H. Meldner, Arkiv Fysik **36**, 593 (1967).
[3] W. D. Mayers and W. J. Swiatecki, Nucl. Phys. **81**, 1 (1966).
[4] S. G. Nilsson *et al.*, Nucl. Phys. A **131**, 1 (1969).
[5] U. Mosel and W. Greiner, Z. Phys. **222**, 261 (1969).
[6] G. T. Seaborg, J. Chem. Educ. **46**, 626 (1969).
[7] S. Hofmann *et al.*, Z. Phys. A **354**, 229 (1996).
[8] S. Hofmann and G. Münzenberg, Rev. Mod. Phys. **72**, 733 (2000); S. Hofmann *et al.*, Eur. Phys. J. A **14**, 147 (2002).
[9] K. Kumar, *Superheavy Elements* (Adam Higler, Bristol, 1989).
[10] Yu. Ts. Oganessian *et al.*, Phys. Rev. Lett. **83**, 3154 (1999).
[11] Yu. Ts. Oganessian *et al.*, Phys. Rev. C **62**, 041604(R) (2000); **63**, 011301 (2000).
[12] Yu. Ts. Oganessian *et al.*, Nucl. Phys. A **685**, 17c (2001).
[13] Yu. Ts. Oganessian *et al.*, Phys. Rev. C **69**, 054607 (2004); **69**, 021601(R) (2004).
[14] Yu. Oganessian, J. Phys. G: Nucl. Part. Phys. **34**, R165 (2007).
[15] R. Eichler *et al.*, Nucl. Phys. A **787**, 373c (2007).
[16] Y. T. Oganessian *et al.*, Phys. Rev. Lett. **104**, 142502 (2010); **108**, 022502 (2012); Y. T. Oganessian, Acta Phys. Pol. B **43**, 167 (2012).
[17] Yu. Ts. Oganessian *et al.*, Phys. Rev. C **83**, 054315 (2011).
[18] S. Hofmann *et al.*, Z. Phys. A **350**, 277 (1995).
[19] S. Hofmann *et al.*, Z. Phys. A **350**, 281 (1995).
[20] S. Hofmann *et al.*, Rep. Prog. Phys. **61**, 639 (1998).
[21] S. Hofmann *et al.*, Acta Phys. Pol. B **30**, 621 (1999).
[22] K. Morita *et al.*, J. Phys. Soc. Jpn. **73**, 2593 (2004).
[23] K. Morita *et al.*, J. Phys. Soc. Jpn. **81**, 103201 (2012).
[24] K. Rutz, M. Bender, T. Bürvenich, T. Schilling, P.-G. Reinhard, J. A. Maruhn, and W. Greiner, Phys. Rev. C **56**, 238 (1997); M. Bhuyan and S. K. Patra, Mod. Phys. Lett. A **27**, 1250173 (2012).
[25] R. K. Gupta, S. K. Patra, and W. Greiner, Mod. Phys. Lett. A **12**, 1727 (1997).
[26] S. K. Patra, C.-L. Wu, C. R. Praharaj, and R. K. Gupta, Nucl. Phys. A **651**, 117 (1999).
[27] A. T. Kruppa, M. Bender, W. Nazarewicz, P.-G. Reinhard, T. Vertse, and S. Ćwiok, Phys. Rev. C **61**, 034313 (2000).
[28] S. Ćwiok, J. Dobaczewski, P.-H. Heenen, P. Magierski, and W. Nazarewicz, Nucl. Phys. A **611**, 211 (1996); S. Ćwiok, W. Nazarewicz, and P. H. Heenen, Phys. Rev. Lett. **83**, 1108 (1999).
[29] S. Ćwiok, P.-H. Heenen, and W. Nazarewicz, Nature **433**, 705 (2005).

[30] W. Zhang, J. Meng, S. Q. Zhang, L. S. Geng, and H. Toki, Nucl. Phys. A **753**, 106 (2005).
[31] R. D. Herzberg *et al.*, Nature (London) **442**, 896 (2006).
[32] A. Marinov, I. Rodushkin, Y. Kashiv, L. Halicz, I. Segal, A. Pape, R. V. Gentry, H. W. Miller, D. Kolb, and R. Brandt, Phys. Rev. C **76**, 021303(R) (2007).
[33] S. K. Patra, M. Bhuyan, M. S. Mehta, and Raj K. Gupta, Phys. Rev. C **80**, 034312 (2009).
[34] Zhongzhou Ren and Hiroshi Toki, Nucl. Phys. A **689**, 691 (2001).
[35] A. Marinov, I. Rodushkin, D. Kolb, A. Pape, Y. Kashiv, R. Brandt, R. V. Gentry, and H. W. Miller, Int. J. Mod. Phys. E **19**, 131 (2010); A. Marinov, I. Rodushkin, A. Pape, Y. Kashiv, D. Kolb, R. Brandt, R. V. Gentry, H. W. Miller, L. Halicz, and I. Segal, *ibid.* **18**, 621 (2009).
[36] G. A. Lalazissis, J. König, and P. Ring, Phys. Rev. C **55**, 540 (1997).
[37] P. G. Reinhard, Rep. Prog. Phys. **52**, 439 (1989).
[38] P. Ring, Prog. Part. Nucl. Phys. **37**, 193 (1996).
[39] D. Vretenar, A. V. Afanasjev, G. A. Lalazissis, and P. Ring, Phys. Rep. **409**, 101 (2005).
[40] J. Meng *et al.*, Prog. Part. Nucl. Phys. **57**, 470 (2006).
[41] Haozhao Liang, Jie Meng, and Shan-Gui Zhou, Phys. Rep. **570**, 1 (2015).
[42] R. Machleidt, Adv. Nucl. Phys. **19**, 189 (1989).
[43] S. K. Patra and C. R. Praharaj, Phys. Rev. C **44**, 2552 (1991).
[44] M. Del Estal, M. Centelles, X. Viñas, and S. K. Patra, Phys. Rev. C **63**, 024314 (2001).
[45] B. D. Serot and J. D. Walecka, Adv. Nucl. Phys. **16**, 1 (1986).
[46] Y. K. Gambhir, P. Ring, and A. Thimet, Ann. Phys. (NY) **198**, 132 (1990).
[47] S. K. Patra, Phys. Rev. C **48**, 1449 (1993).
[48] M. A. Preston and R. K. Bhaduri, in *Structure of Nucleus* (Addison-Wesley, New York, 1982), Chap. 8, p. 309.
[49] D. G. Madland and J. R. Nix, Nucl. Phys. A **476**, 1 (1988).
[50] J. Dechargé and D. Gogny, Phys. Rev. C **21**, 1568 (1980).
[51] P. Möller, J. R. Nix, W. D. Wyers, and W. J. Swiatecki, At. Data Nucl. Data Tables **59**, 185 (1995); P. Möller, J. R. Nix, and K.-L. Kratz, *ibid.* **66**, 131 (1997).
[52] M. S. Mehta, B. K. Raj, S. K. Patra, and R. K. Gupta, Phys. Rev. C **66**, 044317 (2002)
[53] A. A. Saldanha, A. R. Farhan, and M. M. Sharma, J. Phys. G: Nucl. Part. Phys. **36**, 115103 (2009).
[54] S. K. Patra and C. R. Praharaj, J. Phys. G: Nucl. Part. Phys. **23**, 939 (1997).
[55] G. Audi, A. H. Wapstra, and C. Thibault, Nucl. Phys. A **729**, 337 (2003).
[56] V. E. Viola and G. T. Seaborg, J. Inorg. Nucl. Chem. **28**, 741 (1966).
[57] A. Sobiczewiski, Z. Patyk, and S. C. Cwiok, Phys. Lett. B **224**, 1 (1989).
[58] M. Bender, K. Rutz, P.-G. Reinhard, J. A. Maruhn, and W. Greiner, Phys. Rev. C **60**, 034304 (1999).
[59] J. Dechargé, J.-F. Berger, K. Dietrich, and M. S. Weiss, Phys. Lett. B **451**, 275 (1999).
[60] J. C. Pei, F. R. Xu, and P. D. Stevenson, Phys. Rev. C **71**, 034302 (2005).